Effect of Impurities on Emulsion Polymerization: Case I Kinetics

A. PENLIDIS,* J. F. MacGREGOR, and A. E. HAMIELEC,
McMaster Institute for Polymer Production Technology, Department of Chemical Engineering, McMaster University, Hamilton, Ontario, Canada L8S 4L7

Synopsis

The effect of water- and monomer-soluble impurities on the kinetics of emulsion polymerization for Case I systems (e.g., vinyl acetate and vinyl choride) was investigated. Model predictions on the effect of these impurities on polymer particle nucleation and growth rate are shown to be in satisfactory agreement with experimental results. The effect of monomer-soluble impurities is shown to be quite different from that observed in Case II emulsion polymerization systems.

INTRODUCTION

In our previous paper[1] the importance of reactive impurities on industrial emulsion polymerization was discussed. An experimental investigation into the effect of both water- and monomer-soluble impurities on the kinetics of emulsion polymerization for Case II systems (e.g., styrene) revealed that even at low concentrations both types of impurities had a pronounced but very different effect on the particle generation and growth rate. A mathematical model was presented that was capable of predicting these experimentally observed effects.

In this paper we treat Case I systems. These systems, typified by vinyl acetate or vinyl chloride, are characterized by polar monomers that have a moderate solubility in water and a relatively high rate of radical chain transfer to monomer during polymerization. As a result there is a very high rate of desorption of monomeric and oligomeric radicals from the particles and the average number of radicals per particle is therefore much less than half.

WATER-SOLUBLE IMPURITIES

Oxygen, which is the most common impurity that actively scavenges radicals, is soluble in both water and the organic phase. In fact, its solubility in the organic phase is usually much higher. Oxygen is treated herein as a water-soluble impurity (WSI) for the following reasons. Radicals that are generated in the water phase via initiator decomposition are scavenged by oxygen dissolved in the water phase with sufficient rapidity that oligomeriza-

*To whom correspondence should be addressed. Current address: Department of Chemical Engineering, University of Waterloo, Waterloo, Ontario, Canada N2L 3G1.

Journal of Applied Polymer Science, Vol. 35, 2023–2038 (1988)
 CCC 0021-8995/88/082023-16$04.00

tion of initiator radicals does not significantly occur. Oligomer radicals if formed diffuse into the organic particles (monomer-swollen micelles, monomer droplets) and are consumed by oxygen there. This in fact continues until all of the oxygen in the water, micelles, and monomer droplets is consumed. Thereafter the induction period ends and polymerization of high molecular weight chains begins. It is conceivable that oxygen in the headspace gas may continue to slowly diffuse into the water and organic phases even after the end of the induction period, causing some retardation in polymerization rate. This phenomenon is general and should occur in both Case I and Case II systems.

The effects of the most common water-soluble impurities such as dissolved oxygen and inhibitors exhibiting an appreciable solubility in water [e.g., hydroquinone (HDQ)] on the kinetics of Case I systems are similar to what has been observed with Case II systems.[1] These impurities rapidly consume reactive free radicals in the water phase, thereby preventing particle generation and inhibiting the growth of any particles already present. This gives rise to the commonly observed induction period. If the concentration of these reactive impurities is not so great as to consume a substantial portion of the initiator charge, then once the impurities have been consumed the induction period ends, and the reaction usually proceeds in a normal fashion. Similarly, in this case, if for example oxygen is suddenly introduced into the reactor as a slug it will reduce (or stop) the rate of polymerization until it has been consumed by radicals formed by initiator decomposition at which time the reaction will resume its previous course. If introduced into the reactor in sufficient quantities the reaction will completely cease and all the initiator will be consumed ("deadend" polymerization). Only upon reintroduction of sufficient initiator to consume all the impurities will the reaction again proceed. Indeed, recently, oxygen injection has been proposed and experimentally demonstrated as an effective control measure for limiting the rate of heat release and altering the rate of polymerization in emulsion processes.[2] The use of pulse injections of air in commercial microsuspension polymerization reactors has been common practice for years.

Experimental Results

Figure 1 is a plot of emulsion density readings versus time for typical batch poly(vinyl acetate) runs. Details on the recipes and experimental conditions employed can be found elsewhere.[3] The density readings are from an on-line densitometer.[3] The long induction period in run BR4 was caused by oxygen in the reactor which was admitted through a feed valve at the time of charging. The onset of polymerization was indicated by the rather sharp increase in density due to polymer formation. The curves represent density versus time histories for three runs with identical recipes and operating conditions but different amounts of oxygen in the reactor initially. The important point to note is that the only difference among the runs is the duration of the induction period. Once the reaction gets going, the slopes of the three curves and the duration of the reactions are, for all practical purposes, identical.

A reduction in the polymerization rate has been experimentally observed[4] as a consequence of an increase in the oxygen concentration in the water phase during continuous vinyl acetate emulsion polymerization. In all the

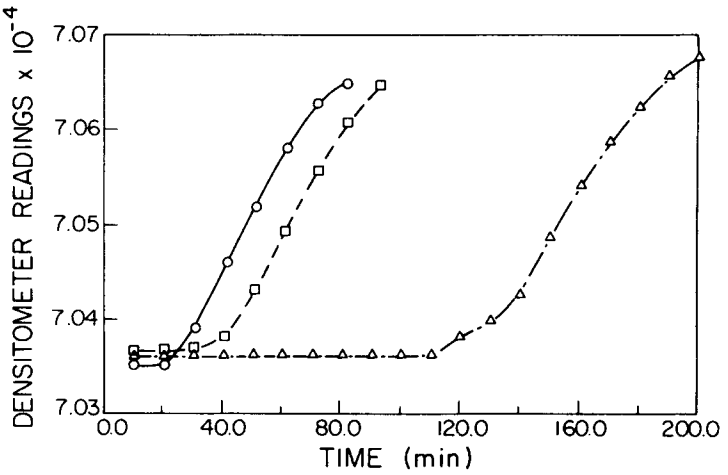

Fig. 1. Effect of oxygen concentration on polymerization rate: Emulsion polymerization of vinyl acetate. (○) BR2; (△) BR4; (▽) BR5.

experiments described by Kiparissides et al.,[4] a certified grade of nitrogen was used for purging the raw materials and the initial reaction mixture. Traces of oxygen were removed by bubbling nitrogen through a 5% pyrogallol solution in 2 mol/L NaOH and then through a silica-gel column for drying. However, some traces of oxygen may have remained in the nitrogen blanket, and some oxygen has diffused through the seals in the agitator shaft. By increasing the agitation rate, a larger liquid–air interface was generated. This increased the oxygen in the water and thus reduced the radical generation rate. The result was a reduction in the polymerization rate and a marked decrease in conversion by ~ 10–15%.

Figure 2 shows conversion versus time results for two batch emulsion poly(vinyl acetate) runs (O1 and O2), during which air was let in the reactor at different points during the experiment. Both runs were isothermal at 50°C with the following recipes: Run O1(water = 3 L, initiator = 3 g, monomer = 1.2 L and emulsifier = 20 g) and Run O2(water = 3 L, initiator = 3 g, monomer = 1.5 L and emulsifier = 15 g). Conversion was determined gravimetrically. At different points, and therefore different conversion levels during the experiment (indicated by the numbered arrows on Fig. 2), a valve on the top of the reactor was opened for short time intervals of different total duration (points (1) and (2) = 90 seconds, point (3) = 120 seconds). Air, and therefore oxygen, was thus allowed to diffuse into the vapor space of the reactor. This oxygen subsequently diffused into the water phase. The final result was a marked reduction in the polymerization rate which caused conversion to level off, as is evident from the conversion-time curves in Figure 2. The duration of the oxygen effect was ~ 12 minutes for point (1), ~ 5 minutes for point (2), and ~ 8 minutes for point (3). The reaction resumed its typical course each time when most of the oxygen in the water phase was consumed by radicals.

As stated earlier, oxygen as an inhibitor does not affect the course of the reaction. Nevertheless, soluble oligomers may form during the inhibition period which may be surface active and may be adsorbed on the latex

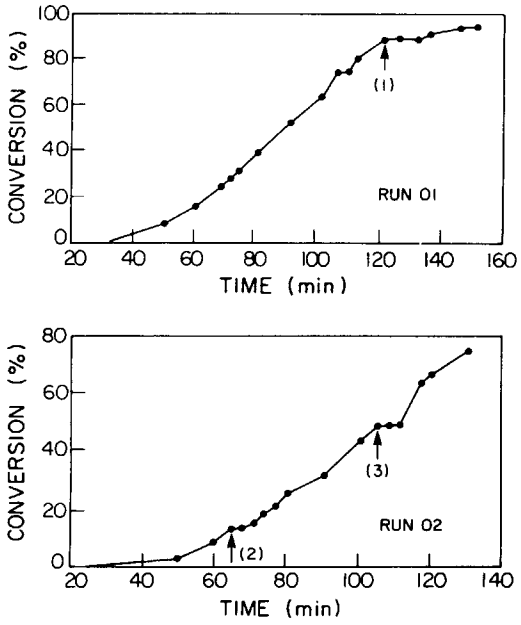

Fig. 2. Effect of oxygen on polymerization rate: Emulsion poly(vinyl acetate).

particles once they form. The effect of this additional "stabilizer" may result in the generation of more particles, and hence give a smaller final particle size compared with that observed in the complete absence of oxygen. Burnett et al.[5] found by a light-scattering method that the average diameter of vinyl acetate particles was 293 nm when vacuum degassing was used, 260 nm when most of the oxygen was displaced with a stream of nitrogen, and 219 nm when the oxygen concentration was increased by passing in oxygen. Similar results have also been observed by Blackley and Haynes.[6]

MONOMER-SOLUBLE IMPURITIES

Modeling the Effect of Impurities

A population balance model for Case I emulsion polymerizations has been developed in Refs. 7 and 8, which has been shown to be capable of predicting the development of particle size, conversion, and molecular weight with time for poly(vinyl acetate)[3,4] and poly(vinyl chloride)[9] in both batch and continuous stirred tank reactors. In this section we consider the necessary modifications to this model to account for the effects of reactive monomer-soluble impurities (MSI).

The model is based on an age distribution analysis which considers classes of particles that are in the reactor at time t, but were born between times τ and $\tau + d\tau$. The number of particles in such a class is denoted by $n(t, \tau)\, d\tau$, and any property of that class by $p(t, \tau)$ (e.g., diameter or area of particles of class (t, τ)). Integration of $n(t, \tau)\, d\tau$ over the time period t will give the total number of particles in the reactor at time t. Also, a total property $P(t)$ (e.g., total particle surface area in the reactor at time t) can be obtained by

summing (integrating) $p(t, \tau)$ over all classes of particles in the reactor vessel, viz:

$$P(t) = \int_0^t p(t, \tau) n(t, \tau)\, d\tau \tag{1}$$

Details about the model development and an explanation of the equations involved can be found in several sources.[3,7-10] A short summary of the parts of the model used in this paper is provided in the Appendix.

To modify this model to account for impurities one must rederive the radical balances in the reactor to include reactions with monomer-soluble impurities. MSI partition between monomer droplets and polymer particles, and scavenge radicals in the polymer particles. Equation (16) for the radical entry rate into a class of particles remains the same as for an impurity-free case, but Eq. (18), the stationary radical balance for the whole class, will now become:

$$R_I(t) \frac{A_n(t, \tau)\, d\tau}{A_p(t)} = 2[\rho(t, \tau) - \rho_{MI}(t, \tau)]\, \bar{q}(t, \tau) + \rho_{MI}(t, \tau) \tag{2}$$

The first term in the RHS of Eq. (2) represents instantaneous termination of radicals which enter polymer particles. The term $\rho_{MI}(t, \tau)$ accounts for the rate of consumption of radicals in polymer particles by reactions with MSI and is given by:

$$\rho_{MI}(t, \tau) = k_{MI}(MI)_p(t) \bar{q}(t, \tau) n(t, \tau)\, d\tau \tag{3}$$

k_{MI} is the rate constant for the reaction of radicals with MSI and $(MI)_p(t)$ represents the concentration of MSI inside the polymer particles. $(MI)_p(t)$ can be related to $(MI)(t)$, the total concentration of MSI in the system, through a partition coefficient as follows:

$$K_{\text{MSI}} = \frac{(MI)_p(t)}{(MI)(t)} \tag{4}$$

Hoffman[15] chose K_{MSI} to be equal to $\Phi(t)$, the monomer volume fraction in the polymer particles, and in the absence of experimental partition coefficients the same assumption is employed in the present analysis. What Eq. (4) basically says is that up to the critical conversion x_c, before monomer droplets disappear, K_{MSI} is constant. After monomer droplets disappear (i.e., for conversion levels $x(t) > x_c$), the MSI resides completely in the polymer particles and $(MI)_p(t)$ is decreasing with time.

Combination of Eqs. (16) and (2) yields a new expression for $\bar{q}(t, \tau)$, the average number of radicals per particle in a given class, which accounts for the consumption of radicals by MSI:

$$\bar{q}(t, \tau) = \Psi_{\text{mod}}(t, \tau) a_p(t, \tau) \tag{5}$$

with

$$\Psi_{\text{mod}}(t, \tau) = \frac{-k_{MI}(MI)_p(t)}{4\pi A} + \frac{1}{4\pi A} \left\{ k_{MI}^2 (MI)_p^2(t) + 8 \frac{\pi A R_I(t)}{A_p(t)} \right\}^{1/2} \tag{6}$$

By comparing Eqs. (21) and (6) one can easily see how the existence of monomer-soluble impurities modifies $\bar{q}(t, \tau)$.

Finally, the material balance for MSI for a continuous process can be written as:

$$\frac{d(MI)(t)}{dt} = \frac{(MI)_F(t)}{\theta} - \frac{(MI)(t)}{\theta} - \frac{k_{MI}(MI)_p(t)N_p(t)\bar{q}(t)}{N_A} \tag{7}$$

where $(MI)_F(t)$ represents the MSI concentration in the feed streams, θ the reactor mean residence time, N_A the Avogadro's number, $N_p(t)$ the total number of polymer particles per liter of latex, and

$$\bar{q}(t) = \left\{ \int_0^t \bar{q}(t, \tau) n(t, \tau)\, d\tau \right\} \Big/ N_p(t) \tag{8}$$

Simulation Studies and Physical Interpretation of the Model Equations

The effect of monomer-soluble impurities on the polymerization kinetics of Case I systems should be quite different from their effect on Case II systems because of the different manner by which they affect both particle growth and particle nucleation. We consider both of these effects in turn.

Effect on particle growth. The rate of polymerization in particles of any class is directly proportional to $\bar{q}(t, \tau)$ [see Eq. (14)]. This term is directly affected by the MSI as shown by Eq. (6). The extent of the MSI effect will depend upon the magnitude of the two terms involving $(MI)_p(t)$ on the right-hand side of Eq. (6) relative to that of the last term which is independent of the MSI. For values of $(k_{MI}(MI)_p(t)) \ll (8\pi A R_I(t)/A_p(t))$ the MSI will have little effect on $\bar{q}(t, \tau)$ and hence on the particle growth rates, while for larger values of $(k_{MI}(MI)_p(t))$ the effect can become substantial. These situations are illustrated in the simulations of Figures 3 and 4.

Figure 3 gives results for the emulsion polymerization of poly(vinyl acetate) in a train of two continuous stirred tank reactors.[10] Conversion from the second reactor is plotted against dimensionless time (t/θ) with a residence time in the second reactor of $\theta = 30$ minutes. Three cases are plotted in Figure 3(a): a case with a constant concentration of both water- and monomer-soluble impurities in the feed stream of 20 ppm, and two other cases where both impurity concentrations were varied by $\pm 50\%$. No discernible effect of the impurities can be observed at this low impurity concentration level. In Figure 3(b) three cases are again plotted: 0, 20, and 200 ppm of MSI. Again there is no discernible effect at low impurity levels (0 and 20 ppm). However, at 200 ppm the MSI have an effect, reducing the conversion by approximately 10% below that for the 0 and 20 ppm cases.

Figure 4 shows the model predictions for conversion, average particle diameter, and MSI concentration for different MSI levels in the batch emulsion polymerization of vinyl acetate. The conversion versus time plots in Figure 4(a) show little difference for low MSI concentrations, but again much larger effects at higher MSI concentrations (100–400 ppm).

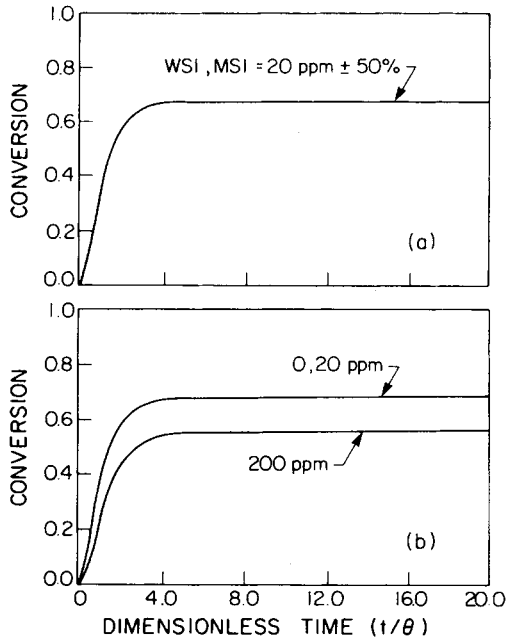

Fig. 3. Simulation results: Continuous latex train conversion vs. (t/θ) for several impurity levels.

In Figures 3 and 4 the rate constant for reaction between MSI and radicals (k_{MI}) was taken to be equal to the propagation rate constant (k_p). Figure 5 shows the effect on the polymerization rate of changing the value of k_{MI}.

Effect on particle nucleation. The MSI have two competing effects influencing the final number of particles generated. Consider the expression for the overall rate of particle nucleation in Case I systems by both homogeneous and micellar mechanisms given by combining Eqs. (9) and (11), that is by

$$f(t) = \rho(t)\frac{k_m A_m(t) k_v + k_h}{k_m A_m(t) k_v + k_h + k_{ab} A_p(t) k_v} \tag{9}$$

The rate at which particles are nucleated and the total number of particles nucleated depend upon the time behavior of the radical entry rate, $\rho(t)$, and the micellar and particle surface areas, $A_m(t)$ and $A_p(t)$, respectively. Typically for Case I polymerizations the particle generation rate is very high and lasts only a few minutes. This is a result of the very high value of $\rho(t)$ given by Eq. (16), in which the contribution from radical desorption $\rho_{des}(t, \tau)$ is usually much larger than that from initiator decomposition $(R_I(t)A_n(t, \tau)\, d\tau/A_p(t))$. From Eq. (17) $\rho_{des}(t, \tau)$ is directly proportional to $\bar{q}(t, \tau)$ which is affected by the MSI through Eqs. (5) and (6). As $(MI)_p(t)$ increases, $\bar{q}(t, \tau)$ and hence $\rho(t)$ will decrease. However, from Eq. (14) the rate of growth of particle volume is also directly proportional to $\bar{q}(t, \tau)$. Hence, as $(MI)_p(t)$ increases, and $\bar{q}(t, \tau)$ falls, the particle surface area, $A_p(t)$, will grow more slowly and the micellar area, $A_m(t)$, will decrease more slowly. The

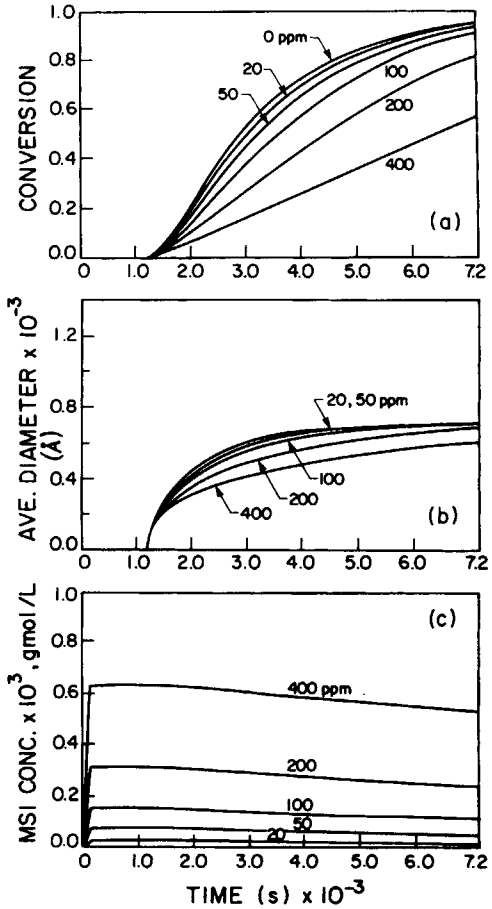

Fig. 4. Simulation results: Batch reactor operation (a) conversion, (b) average diameter, and (c) MSI concentration vs. reaction time for different MSI levels.

particle generation period will therefore be prolonged, and the term multiplying $\rho(t)$ in Eq. (9) will decrease less rapidly in the presence of impurities. The above two effects are compensating in that the former reduces the number of particles generated in a given time while the latter increases the time period for nucleation. The resulting effect is that there may be little change in the total number of particles generated, and hence on the final particle diameters.

The total effect of increasing the MSI level on the rate of particle generation and the number of particles generated is illustrated via simulation in Table I [and Fig. 4(b)] for the batch polymerization of vinyl acetate. The total number of particles generated is very little changed for MSI levels ranging from 0 to 400 ppm.

Experimental Plan

The batch reactor that was used for the impurity runs was identical to the 5 liter stainless steel reactor described by us elsewhere.[3] The vinyl acetate

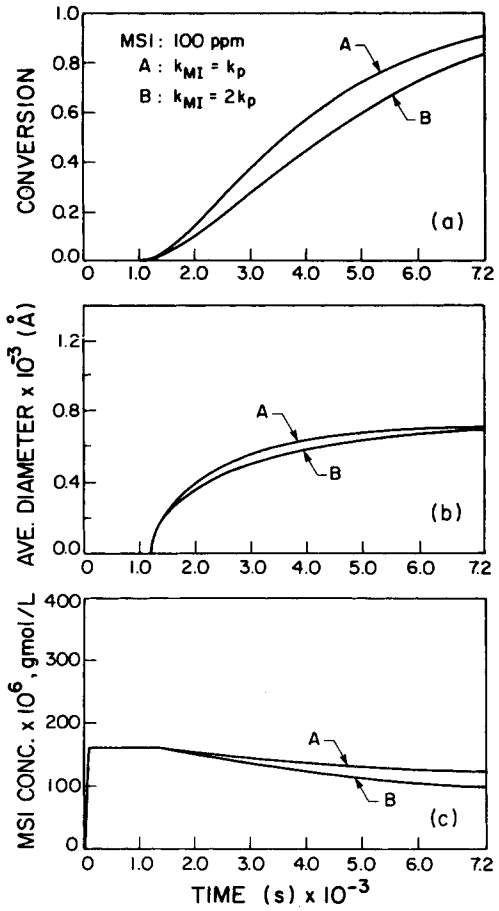

Fig. 5. Simulation results: Batch reactor operation, MSI level of 100 ppm. Effect of k_{MI} on (a) conversion, (b) average particle diameter, and (c) MSI concentration.

monomer was 99 + % pure (Aldrich, catalog number V150-3), inhibited with only 3–5 ppm HDQ. The remaining HDQ was removed prior to polymerization by passing the monomer three times through a bed of Rohm and Haas Amberlyst A-27 ion exchange resin, strongly basic (Aldrich, catalog number 21643–7), using a low flow rate (< 5 mL/min). Water, emulsifier, and initiator

TABLE I
MSI Effect on Number of Particles

MSI concentration (ppm)	Number of particles per liter of latex $\times 10^{-19}$
0	0.110
20	~ 0.110
50	0.115
100	0.120
200	0.128
400	0.133

TABLE II
Summary of Batch VAc Impurity Runs

Run[a]	IM1 (base case)	IM3	IM4	IM5	IM6
TBC (ppm)	—	20	200	100	50

[a] For all runs: VAc = 1150 mL, water = 2860 mL, I = 2.0 g, S = 15.0 g, Temp. = 50°C and HDQ present < 1 ppm.

were as described previously[3] and the 4-*tert*-butyl catechol (TBC) employed as the MSI was BDH ACS (analytical) grade.

Monomer, water, initiator, and emulsifier solutions were all charged into the reactor vessel, the mixture was stirred at 300–320 rpm and 20–25°C while being degassed for ~ 10 minutes, and then the reaction started by raising the temperature to 50°C. Samples were drawn off every 5 minutes. Conversion was determined gravimetrically and particle diameter by hydrodynamic chromatography (HDC). A Corning pH meter 140 was occasionally used to verify pH measurements done on the latex samples by common pH paper indicator.

Table II summarizes the batch vinyl acetate (VAc) runs performed and their operating conditions.

Experimental Results

Figure 6(a) shows results from the impurity-free run IM1 (which will serve as a base case). The pH was close to 6 at the beginning of the run and closer to 5 (~ 5.10) at the final stages. The induction time (due to traces of oxygen) was ~ 1200 s, a very typical value according to the discussion in Ref. 3. The solid line represents model predictions, and as one can clearly see, the agreement between model and experimental conversion is quite good.

The recipe of run IM3, the conversion-time history of which is shown in Figure 6(b), was identical to the one of run IM1, with the extra addition of 20 ppm monomer-soluble TBC. IM3 exhibited about the same induction period as run IM1, a further indication that MSI act in a different way than WSI and do not affect the initial induction periods. (In addition, the fact that IM1 and IM3 exhibited the same induction time was a verification of the good reproducibility of the experimental procedure employed.) The pH during IM3 was again between 6 and 5. The experimental results of Figure 6(b) clearly suggest that an MSI level of 20 ppm does not affect the polymerization rate appreciably, an observation consistent with the previous model predictions.

A comparison between the conversion histories in runs IM3, IM4, IM5, and IM6 is given in Figure 7. A level of 200 ppm TBC (Run IM4) is considered high and can result, in practice, from monomer recycle streams back to the main reactor from downstream monomer recovery units. All four runs gave nearly the same pH levels and induction times as previously. Of course, a more precise interpretation of the results of Figure 7 depends strongly upon having precise estimates of the induction periods. However, one can clearly see the small effect on conversion in the 0–50 ppm cases and the larger effect in the 100–200 ppm range, which is in agreement with the simulations of Figure 4.

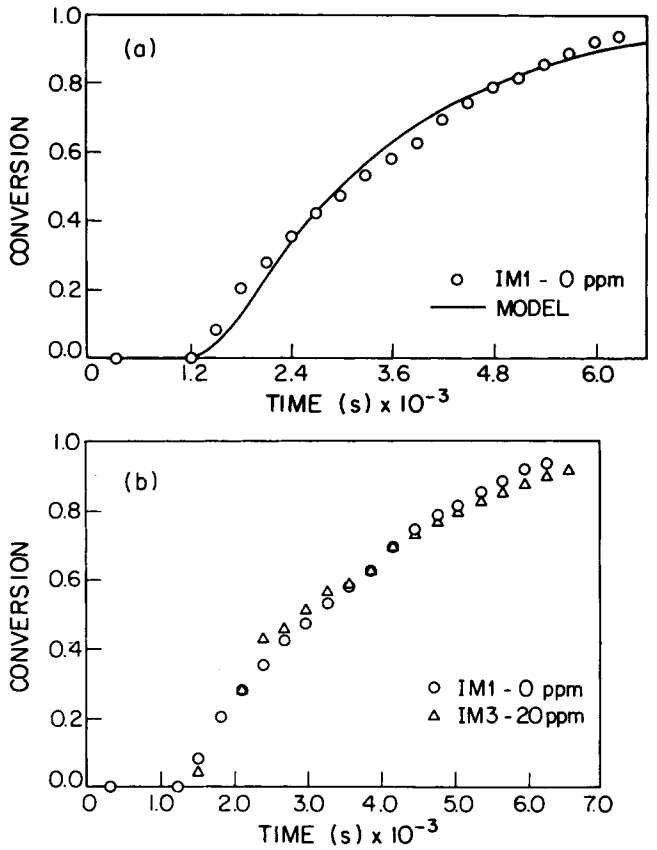

Fig. 6. Conversion-time histories for runs (○) IM1 (0 ppm) and (△) IM3 (20 ppm).

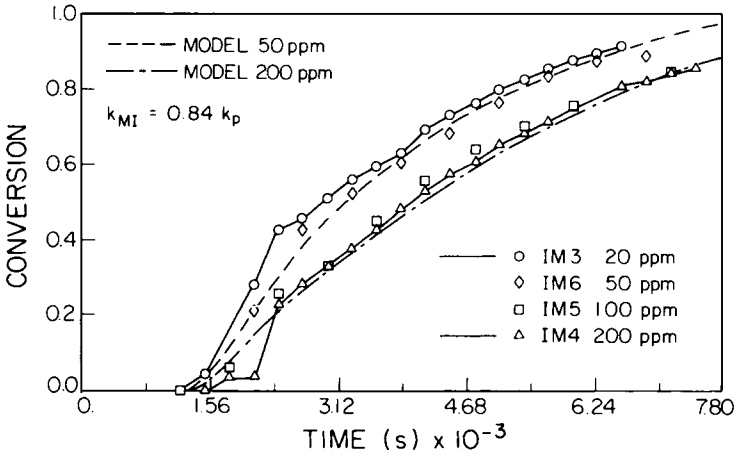

Fig. 7. Conversion-time histories for runs IM3, IM4, IM5, and IM6.

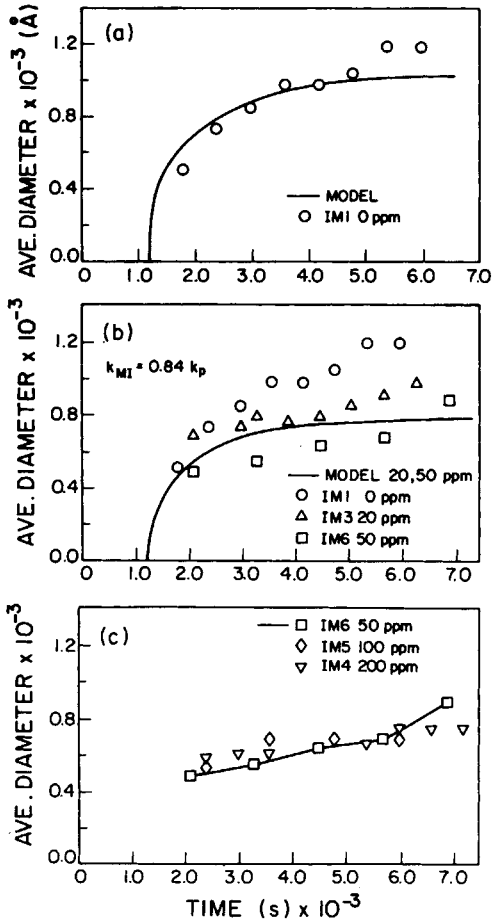

Fig. 8. Average particle diameter vs. batch reaction time for runs IM1, IM3, IM4, IM5, and IM6.

Figure 8 summarizes the average particle diameter histories for runs IM1, IM3, IM4, IM5, and IM6. The average diameters measured (and reported on the plots in angstroms) are coming from HDC and are based on "peak" retention volume.[3,10] As the MSI level increases, particle diameter decreases, but note that for the same final conversion level (~ 85%), the difference in diameter between runs IM3 (20 ppm) and IM6 (50 ppm) is only ~ 25 Å [Fig. 8(b)]. In Figure 8(c), the obtained sizes are somewhat lower than the diameters of IM1 (0 ppm) and lie together roughly in the same range for all three impurity levels.

In order to check the reproducibility of the HDC measurements, a few repeats were run randomly one month apart. The results which were obtained follow: for sample IM4#8, 578, 585, and 580 Å, respectively; for sample IM4#20, 746 and 740 Å; and for sample IM5#8, 685 and 689 Å, respectively.

The obtained experimental results in Figures 6 through 8 were satisfactorily predicted by the mathematical model. The model showed that for reasonably low MSI levels there should be no or very little difference in conversion. For high impurity levels (greater than 100 ppm), it correctly predicted that there

should be a modest difference. At low MSI levels, desorption is still dominant and the difference is negligible [see Eq. (2)]. At high MSI levels, however, $\bar{q}(t)$ decreases [see Eq. (5)], resulting in a subsequent drop in $R_p(t)$ and conversion. As for polymer particle size, the presence of MSI may cause a slight reduction in $\bar{q}(t)$. This combined with the competing effect on $A_p(t)$, as discussed previously, will finally yield particle diameters somewhat lower compared to the ones of the impurity-free case.

CONCLUDING REMARKS

The nature of the effects of reactive water-soluble and monomer-soluble impurities on Case I emulsion polymerization kinetics has been studied. Water-soluble impurities have been shown to produce an induction period proportional to the amount of impurities present, but to have little effect on the subsequent polymerization. Monomer-soluble impurity levels less than 50 ppm have almost no effect on conversion and particle size. Higher levels reduce the polymerization rate and conversion, but they do not affect the rate as appreciably as for Case II systems. The final particle diameter is defined by a competing effect of the MSI on $\bar{q}(t)$ and $A_m(t)$, and is usually lower compared to an impurity-free case. These results were well predicted by a mathematical model that incorporates the effects of impurities.

NOMENCLATURE

d_M, d_p	densities of monomer and polymer, respectively
$d_p(t, \tau)$	particle diameter of the class $n(t, \tau)$
k_{ab}	rate constant for radical capture rate by polymer particles
k_m	rate constant for micellar nucleation
k_v	ratio of emulsion phase over water phase
MW	monomer molecular weight
S_{CMC}	critical micelle concentration
$S_T(t)$	total emulsifier (soap) concentration in the reactor
S_α	area coverage by an emulsifier molecule

APPENDIX

An Expression for the Rate of Particle Nucleation

The generation of new polymer particles in an emulsion system is basically due to two mechanisms: micellar and homogeneous particle nucleation. Then, the rate of particle nucleation, $f(t)$, can be expressed according to (6) as:

$$f(t) = k_m A_m(t)(R_w^{\cdot})k_v + k_h(R_w^{\cdot}) \tag{9}$$

$A_m(t)$, the free micellar area in the system, is defined as:

$$A_m(t) = (S_T(t) - S_{CMC})S_\alpha N_A - A_p(t) \tag{10}$$

Terms or symbols not defined in the text are all explained in the Nomenclature section.

If one makes use of the collision theory to describe radical capture mechanisms, and accepts negligible radical termination in the water phase and inflow/outflow of radicals, then application of the radical stationary-state hypothesis yields the following expression for $(R_w^{\cdot})$, the concentra-

tion of (oligomeric) radicals in the reactor:

$$(R_w^{\cdot}) = \frac{\rho(t)}{k_m A_m(t) k_v + k_h + k_{ab} A_p(t) k_v} \tag{11}$$

where $\rho(t)$ represents the total radical generation (production) rate by both initiation ($\rho_i(t)$) and desorption ($\rho_{des}(t)$).

Expressing the specific homogeneous nucleation rate constant, k_h, according to Ref. 10 and substituting Eq. (11) into Eq. (9), one can finally obtain a general expression for the particle nucleation rate, $f(t)$.[7,8,10]

Total Property Balance Equation

Differentiating Eq. (1) with respect to time and using Leibnitz's rule, one can obtain the evolution of $P(t)$ with time, as follows:

$$\frac{dP(t)}{dt} = \frac{P_{IN}(t)}{\theta} - \frac{P(t)}{\theta} + p(t,t)f(t) + \int_0^t \frac{dp(t,\tau)}{dt} n(t,\tau)\, d\tau \tag{12}$$

Equation (12) simply says that the rate of change of total property $P(t)$ equals the total property inflow minus the total property outflow plus the contribution from nucleation ($p(t, t)$ denotes property at birth, namely, $t = \tau$, which is the same for all particles of the class) plus the contribution from growth in the reactor. For example, if one chooses $P(t)$ to be the total polymer particle volume, $V_p(t)$, then $p(t, t)$ becomes the initial particle volume, $v_p(t, t)$, and $d_p(t,\tau)/dt$ denotes the rate of change of particle volume, $dv_p(t, \tau)/dt$. An expression for $dv_p(t, \tau)/dt$ will be derived shortly.

Particle Size Development: Rate of Change of Polymer Volume

The rate of change of polymer volume in a particle of a certain class born at time τ, now being at time t, is given by the following expression:

$$\frac{dv(t,\tau)}{dt} = R_p(t,\tau)\frac{\mathrm{MW}}{d_p} \tag{13}$$

Considering that one particle from a certain class is representative of the whole class, and that M_p, the concentration of monomer in the polymer particles, is the same for the whole class due to a very fast diffusion of monomer from monomer droplets to polymer particles, Eq. (13) becomes:

$$\frac{dv(t,\tau)}{dt} = \left(\frac{k_p d_M}{N_A d_p}\right)\Phi(t)\bar{q}(t,\tau) \tag{14}$$

with $\Phi(t)$, the monomer volume fraction in the polymer particles, given by

$$\Phi(t) = \frac{1 - x(t)}{1 - x(t)\left(1 - \dfrac{d_M}{d_p}\right)}, \quad x(t) = x_c \quad \text{if } x(t) \le x_c \tag{15}$$

In Eq. (14), $\bar{q}(t, \tau)$ is the average number of radicals per particle of the class (t, τ), and is calculated below.

Average Number of Radicals per Particle

The steady-state radical balance for a representative class of particles viewed in the water phase becomes:

$$\rho(t,\tau) = \rho_{des}(t,\tau) + R_I(t)\frac{A_n(t,\tau)\, d\tau}{A_p(t)} \tag{16}$$

$\rho(t, \tau)$ represents the radical entry rate in the class, and the second term in the RHS of Eq. (16)

the initiation of the class, with $R_I(t)$ being the initiation rate, $(A_n(t, \tau)\, d\tau)$ the area of the class, and $A_p(t)$ the total particle area in the system. $\rho_{des}(t, \tau)$ is the radical desorption rate from the class given by:

$$\rho_{des}(t, \tau) = \bar{q}(t, \tau) k_{de}(t, \tau) n(t, \tau)\, d\tau \tag{17}$$

In Eq. (17), $k_{de}(t, \tau)$ is the desorption rate constant. A water phase termination term has not been included in Eq. (16) as it is usually negligible after the induction period is over (see Ref. 1).

A second steady-state radical balance for the whole class becomes:

$$R_I(t) \frac{A_n(t, \tau)\, d\tau}{A_p(t)} = 2\rho(t, \tau) \bar{q}(t, \tau) \tag{18}$$

with

$$A_n(t, \tau)\, d\tau = a_p(t, \tau) n(t, \tau)\, d\tau \tag{19}$$

and $a_p(t, \tau)$ denoting the surface area of a particle of the class (t, τ).

Elimination of $\rho(t, \tau)$ from Eqs. (16) and (18), use of Eqs. (17) and (19), and the fact that under normal industrial conditions for Case I systems the rate of desorption of radicals is much greater than the term $(R_I(t) A_n(t, \tau)\, d\tau / A_p(t))$ in Eq. (16) yields the following expression for $\bar{q}(t, \tau)$, if one uses an expression for $k_{de}(t, \tau)$ according to Refs. (11), (12), (13) and (14):

$$\bar{q}(t, \tau) = \Psi(t, \tau) a_p(t, \tau) \tag{20}$$

$$\Psi(t, \tau) = \frac{1}{4\pi A} \left\{ 8 \frac{\pi A R_I(t)}{A_p(t)} \right\}^{1/2} \tag{21}$$

$$A = \frac{12 D_w \delta k_{fm}}{m k_p} \tag{22}$$

In Eq. (22), D_w is the diffusion coefficient of monomeric radicals in the water phase, δ a lumped diffusion coefficient for polymeric radicals, m the radical partition coefficient between the particle and water phases, and k_{fm} and k_p the rate constants for transfer to monomer and propagation, respectively.

Rate Expression for Particle Volume

Recalling that

$$v_p(t, \tau) = \frac{v(t, \tau)}{1 - \Phi(t)} \tag{23}$$

the rate of change of particle volume is now obtained as:

$$\frac{dv_p(t, \tau)}{dt} = \frac{1}{1 - \Phi(t)} \frac{dv(t, \tau)}{dt} + \frac{v(t, \tau)}{(1 - \Phi(t))^2} \frac{d\Phi(t)}{dt} \tag{24}$$

The LHS term of Eq. (24) represents the term $(dp(t, \tau)/dt)$ in Eq. (12) and consists of a growth term (first term on the RHS) and a shrinkage term [second term of the RHS of Eq. (24)].

Therefore, the general property balance Eq. (12) eventually becomes for total particle volume:

$$\frac{dV_p(t)}{dt} = \frac{V_{p_{IN}}(t)}{\theta} - \frac{V_p(t)}{\theta} + v_p(t, t) f(t) + \int_0^t \frac{dv_p(t, \tau)}{dt} n(t, \tau)\, d\tau \tag{25}$$

Recalling that

$$v_p(t,\tau) = \frac{\pi}{6} d_p^3(t,\tau) \tag{26}$$

and that

$$a_p(t,\tau) = \pi d_p^2(t,\tau) \tag{27}$$

one can derive similar equations for total particle diameter and surface area. The equation for the total number of particles is very straightforward and is based on Eq. (12) without the growth term.

Finally, the idea of following classes of polymer particles born in the reactor can also be employed for the molecular weight development. One can write differential equations for the live and dead polymer chains in the reactor, including contributions from the following reactions: transfer to monomer, transfer to polymer, transfer to a chain transfer agent, and terminal double-bond polymerization. The result is a series of ordinary differential equations describing the evolution of the leading moments of the molecular weight distribution and the number of branch points per polymer molecule (see Ref. 8).

References

1. B. P. Huo, J. D. Campbell, A. Penlidis, J. F. MacGregor, and A. E. Hamielec, *J. Appl. Polym. Sci.*, **35**, 2009 (1988).

2. B. M. Louie, T. Franaszek, T. Pho, W. Y. Chiu, and D. S. Soong, *J. Appl. Polym. Sci.*, **30**, 3841 (1985).

3. A. Penlidis, J. F. MacGregor, and A. E. Hamielec, *Polym. Proc. Eng.*, **3**, 185 (1985).

4. C. Kiparissides, J. F. MacGregor, and A. E. Hamielec, *CJChE*, **58**, 48 (1980).

5. G. M. Burnett, R. S. Lehrle, D. W. Ovenall, and F. W. Peaker, *J. Polym. Sci.*, **29**, 417 (1958).

6. D. C. Blackley and A. C. Haynes, *Br. Polym. J.*, **9**, 312 (1977).

7. C. Kiparissides, J. F. MacGregor, and A. E. Hamielec, *J. Appl. Polym. Sci.*, **23**, 401 (1979).

8. M. J. Pollock, J. F. MacGregor, and A. E. Hamielec, in ACS Symp. Ser., Vol. 197, T. Provder, Ed., 209 (1981).

9. A. Penlidis, A. E. Hamielec, and J. F. MacGregor, *J. Vinyl Tech.*, **6**, 134 (1984).

10. A. Penlidis, Ph.D. thesis, Dept. of Chemical Engineering, McMaster University (1986).

11. R.M. Fitch and C. H. Tsai, in *Polymer Colloids*, R. M. Fitch, Ed., Plenum Press, New York, 1971, p. 103.

12. M. Harada, M. Nomura, W. Eguchi, and S. Nagata, *J. Chem. Eng. Japan*, **4**, 54 (1971).

13. M. Nomura, M. Harada, K. Nakagawa, E. Eguchi, and S. Nagata, *J. Chem. Eng. Japan*, **4**, 160 (1971).

14. M. Nomura and M. Harada, *J. Appl. Polym. Sci.*, **26**, 17 (1981).

15. T. W. Hoffman, Intensive Short Course on Polymer Reaction Engineering, Dept. of Chemical Engineering, McMaster University, 1985.

Received July 29, 1987
Accepted July 30, 1987